Article

Synthesis and Characterization of 8-Yttrium(III)-Containing 81-Tungsto-8-Arsenate(III), [Y$_8$(CH$_3$COO)(H$_2$O)$_{18}$(As$_2$W$_{19}$O$_{68}$)$_4$(W$_2$O$_6$)$_2$(WO$_4$)]$^{43-}$

Masooma Ibrahim [1,†], Bassem S. Bassil [1,2] and Ulrich Kortz [1,*]

[1] Department of Life Sciences and Chemistry, Jacobs University, P.O. Box 750 561, 28725 Bremen, Germany; E-Mails: bbassil@jacobs-alumni.de (B.S.B.); masooma.ibrahim@kit.edu (M.I.)

[2] Department of Chemistry, Faculty of Sciences, University of Balamand, P.O. Box 100, Tripoli, Lebanon

† Present address: Institute of Nanotechnology, Karlsruhe Institute of Technology (KIT), Hermann-von-Helmholtz Platz 1, 76344 Eggenstein-Leopoldshafen, Germany.

* Author to whom correspondence should be addressed; E-Mail: u.kortz@jacobs-university.de; Fax: +49-421-200 3102; Tel: +49-421-200 3235 (U.K.).

Academic Editors: Greta Ricarda Patzke and Pierre-Emmanuel Car

Abstract: The 8-yttrium(III)-containing 81-tungsto-8-arsenate(III) [Y$_8$(CH$_3$COO)(H$_2$O)$_{18}$(As$_2$W$_{19}$O$_{68}$)$_4$(W$_2$O$_6$)$_2$(WO$_4$)]$^{43-}$ (**1**) has been synthesized in a one-pot reaction of yttrium(III) ions with [*B*-*α*-AsW$_9$O$_{33}$]$^{9-}$ in 1 M NaOAc/HOAc buffer at pH 4.8. Polyanion **1** is composed of four {As$_2$W$_{19}$O$_{68}$} units, two {W$_2$O$_{10}$} fragments, one {WO$_6$} group, and eight Y^{III} ions. The hydrated cesium-sodium salt of **1** (**CsNa-1**) was characterized in the solid-state by single-crystal XRD, FT-IR spectroscopy, thermogravimetric and elemental analyses.

Keywords: yttrium; polyoxometalates; tungsten; structure; high-nuclearity

1. Introduction

Polyoxometalate (POM) chemistry has gained much attention in recent years, due to potential applications in catalysis, magnetism, material science, and even biomedical systems [1–10]. Most of the

work in this area has been focused on $3d$ transition metal-containing derivatives [11–17]. However, also the area of rare earths-containing POMs has undergone a significant expansion in recent years [18–23]. Lanthanide ions usually have larger coordination numbers (8, 9 or more) than d-block metal ions, and exhibit various coordination geometries [24]. In addition, the larger size of these lanthanide ions usually restricts their full incorporation into the lacunary POM sites. Such coordination behavior renders lanthanide ions frequently as linkers of two or more lacunary POM units, forming large structures [18–23,25–27]. Yttrium is formally not a lanthanide, but can be considered as a pseudo-lanthanide, due to its comparable size and coordination number. Lanthanide-containing POMs possess interesting physicochemical properties such as luminescence and magnetism, as well as Lewis acidity relevant for catalysis [28–30]. For example, the terminal, labile coordination sites of the lanthanide (Ln) ions in $[(Ln)(H_2O)_4P_2W_{17}O_{61}]^{6-}$ and $[(Ln)(H_2O)_4PW_{11}O_{39}]^{4-}$ (Ln = Y^{III}, La^{III}, $Eu,^{III}$ Sm^{III}, or Yb^{III}) are known to catalyze aldol and imino Diels−Alder reactions.[29,30]. Mizuno's group has recently reported the high catalytic activity of the yttrium-containing tungstosilicate dimer $[\{Y(H_2O)_2\}_2(\gamma\text{-}SiW_{10}O_{36})_2]^{10-}$ for the cyanosilylation of ketones and aldehydes with trimethylsilyl cyanide (TMS)CN [31,32].
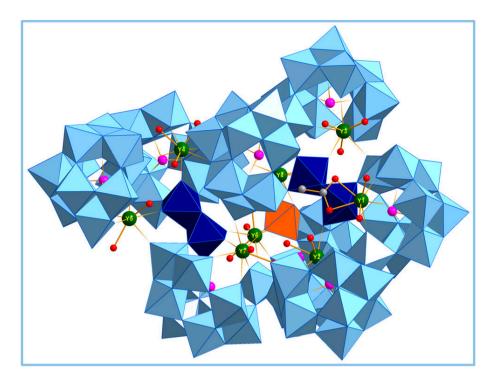
The number of reports on yttrium-containing POMs is significantly lower than for classical lanthanides. In 1971, Peacock and Weakley reported $[Y(W_5O_{18})_2]^{9-}$ [33], which was later used as a catalyst for alcohol oxidations and alkene epoxidations by H_2O_2 [34]. Francesconi's group reported the Y^{III}-containing polyanion $[(PY_2W_{10}O_{38})_4(W_3O_{14})]^{30-}$, which consists of four $[PW_9O_{34}]^{9-}$ units linked by a central $[Y_8W_7O_{30}]^{6+}$ group [35]. Hill and co-workers reported two sandwich-type polyanions, $[(YOH_2)_3(CO_3)(A\text{-}\alpha\text{-}PW_9O_{34})_2]^{11-}$ [36], and $[\{Y_4(\mu_3\text{-}OH)_4(H_2O)_8\}(\alpha\text{-}P_2W_{15}O_{56})_2]^{16-}$ [37]. Very recently, Boskovic's group reported on two Y^{III}-containing polyanions, $[As^{III}_4(Y^{III}W^{VI}_3)W^{VI}_{44}Y^{III}_4O_{159}(Gly)_8(H_2O)_{14}]^{9-}$ and $[As^{III}_4(Mo^{V}_2Mo^{VI}_2)W^{VI}_{44}Y^{III}_4O_{160}(Nle)_9(H_2O)_{11}]^{18-}$, which are functionalized by incorporation of glycine or norleucine [38]. A mixed Ni^{II}-Y^{III}-containing polyanion, $[Y(H_2O)_5\{Ni(H_2O)\}_2As_4W_{40}O_{140}]^{21-}$, based on the large, cyclic POM ligand $[As_4W_{40}O_{140}]^{28-}$ has also been reported [39]. Niu's group reported the solid-state structure of the one-dimensional chain $\{Y(GeW_{11}O_{39})(H_2O)_2\}_n$ [40], composed of Y^{III} and $[GeW_{11}O_{39}]^{8-}$ units. The same group also reported an oxalate-bridged $[\{(\alpha\text{-}PW_{11}O_{39})Y(H_2O)\}_2(C_2O_4)]^{10-}$ [41] and very recently a tartrate-bridged yttrium-containing tungstoarsenate(III) $[\{Y_2(C_4H_4O_6)(C_4H_2O_6)(AsW_9O_{33})\}_2]^{18-}$ [42].

Our group has also been active in the synthesis of novel yttrium-containing POMs. We reported the solid state and solution structure of the Weakley-Peacock type dimer $[YW_{10}O_{36}]^{9-}$, which consists of two monolacunary Lindqvist-based $[W_5O_{18}]^{6-}$ fragments encapsulating a central Y^{III} ion with a square-antiprismatic coordination geometry [43]. Later, we reported the Y^{III}-containing isopolytungstate $[Y_2(H_2O)_{10}W_{22}O_{72}(OH)_2]^{8-}$ as a member of a large family of lanthanide-containing compounds. These isostructural polyanions $[Ln_2(H_2O)_{10}W_{22}O_{72}(OH)_2]^{8-}$ consist of a $\{W_{22}\}$ isopolyanion unit and two lanthanide ions with five terminal water ligands each. [44] We also synthesized the acetate-bridged, dimeric polyanion $[\{Y(\alpha\text{-}GeW_{11}O_{39})(H_2O)\}_2(\mu\text{-}CH_3COO)_2]^{12-}$ [45], as well as the trimeric polyanion $[\{Y(SbW_9O_{31}(OH)_2)(CH_3COO)(H_2O)\}_3(WO_4)]^{17-}$, which is composed of three $\{SbW_9O_{33}\}$ units connected by three Y^{3+} ions and a capping, tetrahedral tungstate group $\{WO_4\}$ [46]. Interestingly, we were also able to encapsulate yttrium(III), and many lanthanide ions, in polyoxopalladates(II), $[Ln^{III}Pd^{II}_{12}(AsPh)_8O_{32}]^{5-}$ (Ln = Y, Pr, Nd, Sm, Eu, Gd, Tb, Dy, Ho, Er, Tm, Yb, Lu). These cuboid-shaped polypalladates(II) are composed of a Pd_{12}-oxo cage, capped by eight phenylarsonate heterogroups, and encapsulating a central guest ion Ln [47]. As part of our continuous
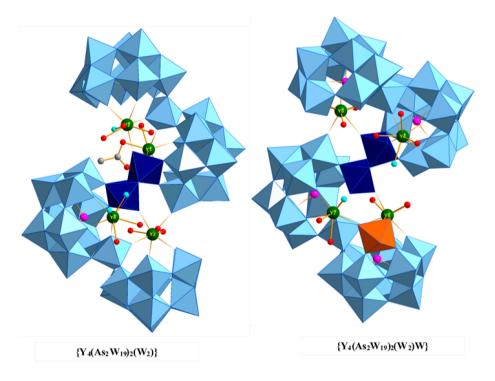
effort to incorporate yttrium(III) ions in POMs, we describe herein the synthesis and structural characterization of an 8-yttrium(III)-containing 81-tungsto-8-arsenate(III).

2. Results and Discussion

Synthesis and Structure. The polyanion $[Y_8(CH_3COO)(H_2O)_{18}(As_2W_{19}O_{68})_4(W_2O_6)_2(WO_4)]^{43-}$ (**1**) has been synthesized using a simple, one-pot procedure by reacting the trilacunary POM precursor $[B\text{-}\alpha\text{-}AsW_9O_{33}]^{9-}$ with Y^{III} ions in 1 M NaOAc/AcOH buffer at pH 4.8, and was characterized in the solid state by IR spectroscopy, as well as thermogravimetric and elemental analysis. The title polyanion crystallizes as a hydrated mixed sodium-cesium salt (**CsNa-1**) in the triclinic space group $P\bar{1}$. Single-crystal XRD on **CsNa-1** revealed that polyanion **1** is composed of four $\{As_2W_{19}O_{68}\}$ units, two $\{W_2O_{10}\}$ fragments, one $\{WO_6\}$ group, and eight yttrium(III) ions (see Figures 1 and 2). The mono- and di-tungsten fragments are most likely formed *in situ* by fragmentation of some of the lacunary $[AsW_9O_{33}]^{9-}$ precursor during the course of the reaction, also seen previously for other large POM architectures [18,21]. The $\{As_2W_{19}\}$ units, also formed *in situ*, are composed of two $\{AsW_9\}$ units connected by an octahedral $\{WO_6\}$ group via corner-shared oxo-bridges. The structure of the $\{As_2W_{19}\}$ units in **1** is different from the known $[As_2W_{19}O_{67}(H_2O)]^{14-}$ POM precursor, where the linking tungsten center has terminal *trans*-oxo-aqua ligands [48]. The linking tungsten(VI) in **1** bridges the two $\{AsW_9\}$ units in a way that the terminal oxo groups are *cis* to each other, non-protonated, and linking the tungsten(VI) to two Y^{III} ions. A total of eight such oxo-bridges are present in **1**, corresponding to the number of yttrium(III) ions. These yttrium(III) ions are all eight-coordinate with distorted square-antiprismatic coordination geometries and Y–O bond distances in the range of 2.3–2.5 Å. The coordination sphere of each Y^{III} center is composed of bridging oxo and terminal aqua ligands (*vide infra*). Two $\{Y_2As_2W_{19}\}$ units are linked to each other by an edge-shared $\{W_2O_6\}$ group to form two dimeric subunits (see Figures 1 and 2). Finally, a tungsten center (W81, corresponding to the orange octahedron in Figures 1 and 2) links the two subunits to each other via two W-O-W (namely to W79 and W80) and four W-O-Y bridges (one to Y6 and Y7, and two to Y8), leading to a 'dimer of dimers'-type assembly. The two subunits are also linked by two Y-O-W bridges, namely Y7-O-W30 and Y4-O-W25. The yttrium centers are all octa-coordinated as stated above, with the coordination sphere filled by Y-O-W bridges or terminal oxo ligands. The two bridging yttriums Y7 and Y8, which are connected to W81, have two terminal aqua ligands each. The rest of the yttrium ions, apart from Y1, have three terminal aqua ligands each. For Y1, an acetate group (from the buffer medium) and two aqua ligands complete the coordination sphere. The existence of such kind of acetate groups has been previously observed, for example in $[Gd_6As_6W_{65}O_{229}(OH)_4(H_2O)_{12}(OAc)_2]^{38-}$ and $[Yb_{10}As_{10}W_{88}O_{308}(OH)_8(H_2O)_{28}(OAc)_4]^{40-}$ [18]. Bond valence sum (BVS) calculations indicate that no bridging oxygen atoms in **1** are protonated [49]. The total charge of **1** is therefore 43-, and is balanced in the solid state by 34.5 sodium and 8.5 cesium counter cations, hence resulting in the formula unit $Cs_{8.5}Na_{34.5}[Y_8(CH_3COO)(H_2O)_{18}(As_2W_{19}O_{68})_4(W_2O_6)_2(WO_4)]\cdot230H_2O$. This formula is supported by elemental and thermogravimetric analyses (see Figure 3).

Figure 1. Combined polyhedral/ball-and-stick representation of **1.** Color code: WO_6 octahedra pale blue/dark blue/orange, As pink balls, Y green balls, O red balls, C grey balls.

$\{Y_4(As_2W_{19})_2(W_2)\}$

$\{Y_4(As_2W_{19})_2(W_2)W\}$

Figure 2. Combined polyhedral/ball-and-stick representation of the two half-units in **1.** The turquoise balls represent bridging oxygens (O_{bridge}). The color code is the same as in Figure 1.
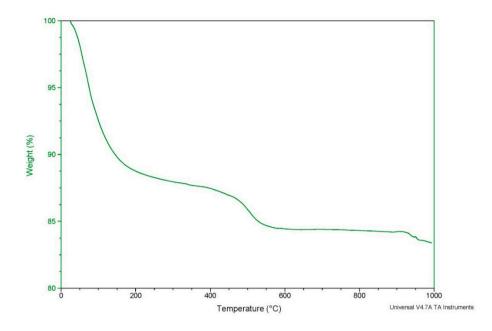
Figure 3. Thermogram of **CsNa-1** from room temperature to 1000 °C.

The synthetic procedure of **1** contains several crucial parameters. An excess of yttrium ions over and above the stoichiometric ratio was needed for optimal yield. Furthermore, the type and pH of the buffer are essential for obtaining the desired product, as well as the presence of cesium ions. In fact, **1** could not be isolated in the absence of cesium ions, and a sufficient amount was needed to induce precipitation, before filtration and crystallization of the product salt. On the other hand, **CsNa-1** proved to be only slightly soluble in D_2O, and hence our solution studies by ^{183}W and ^{89}Y NMR spectroscopy were unsuccessful. NMR measurements on a freshly prepared reaction solution also remained inconclusive. Attempts to prepare isostructural lanthanide derivatives of **1** resulted in reported structures [20]. Finally, to the best of our knowledge, **1** incorporates the largest number of yttrium ions, together with Francesconi's $[(PY_2W_{10}O_{38})_4(W_3O_{14})]^{30-}$ [35]. Boscovic's penta- and tetra-yttrium-containing $[As^{III}_4(Y^{III}W^{VI}_3)W^{VI}_{44}Y^{III}_4O_{159}(Gly)_8(H_2O)_{14}]^{9-}$ and $[As^{III}_4(Mo^V_2Mo^{VI}_2)W^{VI}_{44}Y^{III}_4O_{160}(Nle)_9(H_2O)_{11}]^{18-}$, respectively, should also be mentioned here [38].

Infrared Spectroscopy. The Fourier transform infrared (FTIR) spectrum of **CsNa-1** (see Figure 4) displays a fingerprint region characteristic for the tungsten-oxo framework, indicating the presence of $\{AsW_9\}$ units. The bands in the range of 940–945 cm^{-1} are associated with the antisymmetric stretching vibrations of the terminal W=O bonds, whereas the bands in the range of 850–900 cm^{-1} can be mainly attributed to the antisymmetric stretching vibrations of the As–O(W). The two bands at about 780 cm^{-1} and 700 cm^{-1} arise from antisymmetric stretching of the W–O(W) bridges, whereas the bands below 650 cm^{-1} are due to bending vibrations of the As–O(W) and the W–O(W) bridges [50]. Furthermore, the bands in the range of 1350 – 1620 cm^{-1} can be assigned to vibrations of the bridging acetate group in the polyanion. The broad band at 3440 cm^{-1} and the strong one at 1620 cm^{-1} correspond to crystal waters.

Thermogravimetric Analysis. Thermogravimetric analysis of **CsNa-1** was performed between 25 and 1000 °C under a nitrogen atmosphere to determine the number of crystal waters (see Figure 3). The weight loss of about 92% between 25 and 230 °C can be assigned to the loss of 230 crystal waters per formula unit. In addition, the second continuous weight loss step from 250 to 550 °C corresponds to the removal of 18 coordinated water molecules and decomposition of the acetate group.

3. Experimental Section

General Methods and Materials. All reagents were used as purchased without further purification. The trilacunary POM precursor $Na_9[B\text{-}\alpha\text{-}AsW_9O_{33}]\cdot27H_2O$ was prepared according to the published procedure, and its purity was confirmed by infrared spectroscopy. [51].

Synthesis of $Cs_{8.5}Na_{34.5}[Y_8(CH_3COO)(H_2O)_{18}(As_2W_{19}O_{68})_4(W_2O_6)_2(WO_4)]\cdot230H_2O$ (CsNa-1): 0.50 g (0.20 mmol) $Na_9[B\text{-}\alpha\text{-}AsW_9O_{33}]\cdot27H_2O$ and 0.18 g (0.60 mmol) YCl_3 were added to 20 mL of 1 M NaOAc/HOAc buffer at pH 4.8. The solution was heated to 80 °C for 60 min, cooled to room temperature, and then filtered. Addition of five drops 1.0 M CsCl solution to the filtrate resulted in a precipitate. The reaction mixture was kept at 30 °C for 5 min, and then filtered. The clear colorless filtrate was kept in an open vial at room temperature for slow evaporation. After one week, a colorless crystalline product started to appear. Evaporation was allowed to continue until about half the solvent had evaporated. The solid product was then collected by filtration and air-dried. Yield: 0.25 g (38%). IR (2% KBr pellet, ν/cm^{-1}): 1623(s), 949 (m), 864(s), 788(m), 707(m), 454 (w) (see Figure 4). Elemental analysis for $Cs_{8.5}Na_{34.5}[Y_8(CH_3COO)(H_2O)_{18}(As_2W_{19}O_{68})_4(W_2O_6)_2(WO_4)]\cdot230H_2O$ (**CsNa-1**), calcd. (found): Na 2.91% (2.72%), Cs 4.14 (3.90%) As 2.20% (2.09%), Y 2.61% (2.87%), W 54.7% (55.2%).
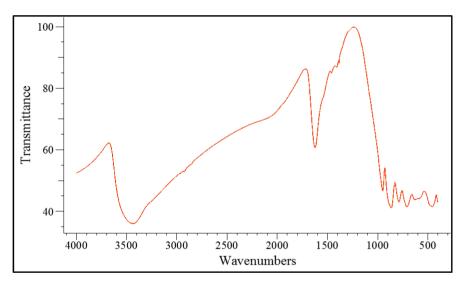

Figure 4. Infrared spectrum of **CsNa-1**.

Instrumentation (IR, TGA). Infrared spectra were recorded on a Nicolet Avatar 370 FT-IR spectrophotometer using KBr pellets. The following abbreviations were used to assign the peak intensities: w = weak, m = medium and s = strong. Thermogravimetric analyses were carried out on a TA Instruments SDT Q600 thermobalance with a 100 mL/min flow of nitrogen; the temperature was ramped from 20 to 1000 °C at a rate of 5 °C /min. Elemental analysis for **CsNa-1** was performed by CNRS, Service Central d'Analyze, Solaize, France.

X-ray Crystallography. A single crystal of **CsNa-1** was mounted on a Hampton cryoloop in light oil for data collection at 173 K. Indexing and data collection were performed on a Bruker D8 SMART APEX II CCD diffractometer with kappa geometry and Mo-Kα radiation (graphite monochromator, λ = 0.71073 Å). Data integration was performed using SAINT [52]. Routine Lorentz and polarization corrections were applied. Multiscan absorption corrections were performed using SADABS [53]. Direct

methods (SHELXS97) successfully located the tungsten atoms, and successive Fourier syntheses (SHELXL2014) revealed the remaining atoms [54]. Refinements were full-matrix least-squares against $|F^2|$ using all data. In the final refinement, all non-disordered heavy atoms (As, W, Y, Cs, Na) were refined anisotropically; oxygen atoms and disordered counter cations were refined isotropically. No hydrogen atoms were included in the models. Crystallographic data are summarized in Table 1. We observed an extra W atom (W82) with an occupancy of 16.67%, but could not model its coordination environment due to serious disorder (see CIF file for details). This result implies that there is a small amount of $\{Y_8As_8W_{82}\}$ polyanion impurity present, which we could not avoid during synthesis or eliminate afterwards, in spite of many attempts.

Table 1. Crystal Data for **CsNa-1**.

Formula	$Cs_{8.5}Na_{34.5}[Y_8(CH_3COO)(H_2O)_{18}(As_2W_{19}O_{68})_4(W_2O_6)_2(WO_4)]\cdot$ $230H_2O$
Formula weight, g/mol	27260.36
Crystal system	Triclinic
Space group	$P\bar{1}$
a, Å	21.7759(5)
b, Å	32.0368(7)
c, Å	33.0799(8)
α, °	94.1720(10)
β, °	107.5370(10)
γ, °	90.5610(10)
Volume, Å^3	21934.4(9)
Z	2
D_{calc}, g/cm^3	4.127
Absorption coefficient	23.661
F(000)	24464
Crystal size, mm	$0.281 \times 0.16 \times 0.126$
Theta range for data collection, °	3.406–23.257
Completeness to Θ_{max}, %	99.6
Index ranges	$-24 \leqslant h \leqslant 24$ $-35 \leqslant k \leqslant 33$ $-36 \leqslant l \leqslant 36$
Total Reflections	651748
Independent Reflections	62815
Calculated Reflections ($I > 2\sigma$)	49552
R(int)	0.0411
Data / restraints / parameters	62815/0/2553
Goodness-of-fit on F2	1.005
R_1 [a]	0.0643
wR_2 [b]	0.1719
Highest / deepest electron density	5.239/−5.002

[a] $R_1 = \sum ||F_o| - |F_c|| / \sum |F_o|$. [b] $wR_2 = [\sum w (F_o^2 - F_c^2)^2/\sum w(F_o^2)^2]^{1/2}$.

4. Conclusions

In conclusion, we have synthesized the 8-yttrium(III)-containing 81-tungsto-8-arsenate(III) $[Y_8(CH_3COO)(H_2O)_{18}(As_2W_{19}O_{68})_4(W_2O_6)_2(WO_4)]^{43-}$ (**1**) using a simple, one-pot procedure by reacting the trilacunary POM precursor $[B\text{-}\alpha\text{-}AsW_9O_{33}]^{9-}$ with Y^{3+} ions in 1 M NaOAc/AcOH buffer at pH 4.8. Polyanion **1** was characterized in the solid state by IR spectroscopy, single crystal XRD, and thermogravimetric analysis. The title polyanion demonstrates the ability of yttrium(III) to act as an efficient linker of POM subunits resulting in large, discrete assemblies. The yttrium(III) ions in **1** possess labile terminal aqua ligands, which allow for Lewis acid type catalysis.

Acknowledgements

Author Contributions

UK proposed the research project and planned for the publication. The manuscript was written by MI and BSB, and then edited by UK. MI performed the lab experiments and BSB did the X-ray diffraction measurements.

Conflicts of Interest

The authors declare no conflict of interest.

References

1. Pope, M.T. *Heteropoly and Isopoly Oxometalates*; Springer: Berlin, Germany, 1983.
2. Pope, M.T.; Müller, A. Polyoxometalate chemistry: An old field with new dimensions in several disciplines. *Angew. Chem., Int. Ed. Engl.* **1991**, *30*, 34–48.
3. Hasenknopf, B.; Micoine, K.; Lacôte, E.; Thorimbert, S.; Malacria, M.; Thouvenot, R. Chirality in polyoxometalate chemistry. *Eur. J. Inorg. Chem.* **2008**, 5001–5013.
4. Kortz, U.; Müller, A.; van Slageren, J.; Schnack, J.; Dalal, N.S.; Dressel, M. Polyoxometalates: Fascinating structures, unique magnetic properties. *Coord. Chem. Rev.* **2009**, *253*, 2315–2327.
5. Kortz, U. Special Issue: Polyoxometalates; John Wiley & Sons, Inc.: Weinheim, Germany, 2009, Volume 34, 5055–5276.
6. Long, D.L.; Tsunashima, R.; Cronin, L. Polyoxometalates: Building blocks for functional nanoscale systems. *Angew. Chem. Int. Ed.* **2010**, *49*, 1736–1758.

7. Izarova, N.V.; Pope, M.T.; Kortz, U. Noble metals in polyoxometalates. *Angew. Chem. Int. Ed.* **2012**, *51*, 9492–9510.

8. Clemente-Juan, J.M.; Coronado, E.; Gaita-Ariño, A. Magnetic polyoxometalates: From molecular magnetism to molecular spintronics and quantum computing. *Chem. Soc. Rev.* **2012**, *41*, 7464–7478.

9. Lv, H.; Geletii, Y.V.; Zhao, C.; Vickers, J.W.; Zhu, G.; Luo, Z.; Song, J.; Lian, T.; Musaev, D.G.; Hill, C.L. Polyoxometalate water oxidation catalysts and the production of green fuel. *Chem. Soc. Rev.* **2012**, *41*, 7572–7589.

10. Pope, M.T.; Kortz, U. Polyoxometalates. In *Encyclopedia of Inorganic and Bioinorganic Chemistry*; Scott, R.A., Ed.; John Wiley: Chichester, UK, 2012.

11. Fang, X.K.; Kögerler, P. PO_4^{3-}-mediated polyoxometalate supercluster assembly. *Angew. Chem. Int. Ed.* **2008**, *47*, 8123–8126.

12. Bassil, B.S.; Ibrahim, M.; Al-Oweini, R.; Asano, M.; Wang, Z.; van Tol, J.; Dalal, N.S.; Choi, K.-Y.; Biboum, R.N.; Keita, B.; Nadjo, L.; Kortz, U. A Planar $\{Mn_{19}(OH)_{12}\}^{26+}$ Unit Incorporated in a 60-Tungsto-6-Silicate Polyanion. *Angew. Chem. Int. Ed.* **2011**, *50*, 5961–5964.

13. Ibrahim, M.; Lan, Y.; Bassil, B.S.; Xiang, Y.; Suchopar, A.; Powell, A.K.; Kortz, U. Hexadecacobalt(II)-containing polyoxometalate-based single-molecule magnet. *Angew. Chem. Int. Ed.* **2011**, *50*, 4708–4711.

14. Zheng, S.–T.; Yang, G.–Y. Recent advances in paramagnetic-TM-substituted polyoxometalates (TM = Mn, Fe, Co, Ni, Cu). *Chem. Soc. Rev.* **2012**, *41*, 7623–7646.

15. Oms, O.; Dolbecq, A.; Mialane, P. Diversity in structures and properties of 3d-incorporating polyoxotungstates. *Chem. Soc. Rev.* **2012**, *41*, 7497–7536.

16. Ibrahim, M.; Xiang, Y.; Bassil, B.S.; Lan, Y.; Powell, A.K.; de Oliveira, P.; Keita, B.; Kortz, U. Synthesis, Magnetism, and Electrochemistry of the Ni_{14}- and Ni_5-Containing Heteropolytungstates $[Ni_{14}(OH)_6(H_2O)_{10}(HPO_4)_4(P_2W_{15}O_{56})_4]^{34-}$ and $[Ni_5(OH)_4(H_2O)_4(\beta\text{-}GeW_9O_{34})(\beta\text{-}GeW_8O_{30}(OH))]^{13-}$. *Inorg. Chem.* **2013**, *52*, 8399–8408.

17. Ibrahim, M.; Haider, A.; Lan, Y.; Bassil, B.S.; Carey, A.M.; Liu, R.; Zhang, G.; Keita, B.; Li, W.; Kostakis, G.E.; Powell, A.K.; Kortz, U. Multinuclear cobalt(II)-containing heteropolytungstates: structure, magnetism, and electrochemistry. *Inorg. Chem.* **2014**, *53*, 5179–5188.

18. Hussain, F.; Gable, W.R.; Speldrich, M.; Kögerler, P.; Boscovic, C. Polyoxotungstate-encapsulated Gd_6 and Yb_{10} complexes. *Chem. Commun.* **2009**, 328–330.

19. Hussain, F.; Conrad, F.; Patzke, G.R. A Gadolinium-bridged polytungstoarsenate(III) nanocluster: $[Gd_8As_{12}W_{124}O_{432}(H_2O)_{22}]^{60-}$. *Angew. Chem. Int. Ed.* **2009**, *48*, 9088−9091.

20. Hussain, F.; Spingler, B.; Conrad, F., Speldrich, M., Kögerler, P.; Boskovic, C.; Patzke, G.R. Cesium-templated lanthanoid-containing polyoxotungstates. *Dalton Trans.* **2009**, 4423–4425.

21. Ritchie, C.; Moore, E.G.; Speldrich, M.; Kögerler, P.; Boskovic, C. Terbium polyoxometalate organic complexes: correlation of structure with luminescence properties. *Angew. Chem. Int. Ed.* **2010**, *49*, 7702–7705.

22. Ritchie, C.; Miller, C.E.; Boskovic, C. The generation of a novel polyoxometalate-based 3D framework following picolinate-chelation of tungsten and potassium centres. *Dalton Trans.* **2011**, *40*, 12037–12039.

23. Ritchie, C.; Baslon, V.; Moore, E.G.; Reber, C.; Boskovic, C. Sensitization of lanthanoid luminescence by organic and inorganic ligands in lanthanoid-organic-polyoxometalates. *Inorg. Chem.* **2012**, *51*, 1142–1151.

24. Cotton, S.A. Lanthanides: Comparison to 3d metals. In *Encyclopedia of inorganic and Bioinorganic Chemistry*; Wiley: Weinheim, Germany, 2012.

25. Wassermann, K.; Dickman, M.H.; Pope, M.T. Self-Assembly of supramolecular polyoxometalates: The compact, water-soluble heteropolytungstate Anion $[As^{III}_{12}Ce^{III}_{16}(H_2O)_{36}W_{148}O_{524}]^{76-}$. *Angew. Chem. Int. Ed. Engl.* **1997**, *36*, 1445–1448.

26. Bassil, B.S.; Dickman, M.H.; Römer, I.; von der Kammer, B.; Kortz, U. The tungstogermanate $[Ce_{20}Ge_{10}W_{100}O_{376}(OH)_4(H_2O)_{30}]^{56-}$: A polyoxometalate containing 20 cerium(III) Atoms. *Angew. Chem. Int. Ed.* **2007**, *46*, 6192–6195.

27. Reinoso, S.; Giménez-Marqués, M., Galán-Mascarós, J.R.; Vitoria, P.; Gutiérrez-Zorrilla, J.M. Giant crown-shaped polytungstate formed by self-assembly of Ce^{III}-stabilized dilacunary Keggin fragments. *Angew. Chem. Int. Ed.* **2010**, *49*, 8384–8388.

28. AlDamen, M.A.; Clemente-Juan, J.M.; Coronado, E.; Martí-Gastaldo, C.; Gaita-Ariňo, A. Mononuclear lanthanide single-molecule magnets based on polyoxometalates. *J. Am. Chem. Soc.* **2008**, *130*, 8874–8875.

29. Boglio, C.; Lemiére, G.; Hasenknopf, B.; Thorimbert, S.; Lacôte, E.; Malacria, M. Lanthanide complexes of the monovacant Dawson polyoxotungstate $[\alpha_1\text{-}P_2W_{17}O_{61}]^{10-}$ as selective and recoverable Lewis acid catalysts. *Angew. Chem. Int. Ed.* **2006**, *45*, 3324−3327.

30. Dupre, N.; Remy, P.; Micoine, K.; Boglio, C.; Thorimbert, S.; Lacôte, E.; Hasenknopf, B.; Malacria, M. Chemoselective catalysis with organosoluble Lewis acidic polyoxotungstates. *Chem. Eur. J.* **2010**, *16*, 7256−7264.

31. Kikukawa, Y.; Suzuki, K.; Sugawa, M.; Hirano, T.; Kamata, K.; Yamaguchi, K.; Mizuno, N. Cyanosilylation of carbonyl compounds with trimethylsilyl cyanide catalyzed by an Yttrium-pillared silicotungstate dimer. *Angew. Chem. Int. Ed.* **2012**, *51*, 3686−3690.

32. Suzuki, K.; Sugawa, M.; Kikukawa, Y.; Kamata, K.; Yamaguchi, K.; Mizuno, N. Strategic design and refinement of Lewis acid–base catalysis by rare-earth-metal-containing polyoxometalates. *Inorg. Chem.* **2012**, *51*, 6953–6961.

33. Peacock, R.D.; Weakley, T.J. R. Heteropolytungstate complexes of the lanthanide elements. Part I. Preparation and reactions. *J. Chem. Soc. A* **1971**, 1836–1839.

34. Griffith, W.P.; Morley-Smith, N.; Nogueira, H.I. S.; Shoair, A.G. F.; Suriaatmaja, M.; White, A.J. P.; Williams, D.J. Studies on polyoxo and polyperoxo-metalates: Part 7. Lanthano- and thoriopolyoxotungstates as catalytic oxidants with H_2O_2 and the X-ray crystal structure of $Na_8[ThW_{10}O_{36}]\cdot 28H_2O$. *J. Organomet. Chem.* **2000**, *607*, 146–155.

35. Howell, R.C.; Perez, F.G.; Horrocks, W.D.; Jain, S.; Rheingold, A.L.; Francesconi, L.C. A new type of heteropolyoxometalates formed from lacunary polyoxotungstate ions and europium or yttrium cations. *Angew. Chem. Int. Ed.* **2001**, *40*, 4031–4034.

36. Fang, X.; Anderson, M.T.; Neiwert, W.A.; Hill, C.L. Yttrium polyoxometalates. synthesis and characterization of a carbonate-encapsulated sandwich-type complex. *Inorg. Chem.* **2003**, *42*, 8600–8602.

37. Fang, X.; Anderson, T.M.; Benelli, C.; Hill, C.L. Polyoxometalate-supported Y– and Yb[III]– hydroxo/oxo clusters from carbonate-assisted hydrolysis. *Chem. Eur. J.* **2005**, *11*, 712–718.

38. Vonci, M. Akhlaghi Bagherjeri, F.; Hall, P.D.; Gable, R.W.; Zavras, A.; O'Hair, R.A. J.; Liu, Y.; Zhang, J.; Field, M.R.; Taylor, M.B.; Du Plessis, J.; Bryant, G.; Riley, M.; Sorace, L.; Aparicio, P.A.; López, X.; Poblet, J.M.; Ritchie, C.; Boskovic, C. Modular molecules: Site-selective metal substitution, photoreduction, and chirality in polyoxometalate hybrids. *Chem. Eur. J.* **2014,** *20*, 14102–14111.

39. Xue, G.; Liu, B.; Hua, H.; Yang, J.; Wang, J.; Fu, F. Large heteropolymetalate complexes formed from lanthanide (Y, Ce, Pr, Nd, Sm, Eu, Gd), nickel cations and cryptate $[As_4W_{40}O_{140}]^{28-}$ synthesis and structure characterization. *J. Mol. Str.* **2004**, *690*, 95–103.

40. Wang, J.P.; Duan, X.Y.; Du, X.D.; Niu, J.Y. Novel rare earth germanotungstates and organic hybrid derivatives: Synthesis and structures of $M/[\alpha-GeW_{11}O_{39}]$ (M = Nd, Sm, Y, Yb) and $Sm/[\alpha-GeW_{11}O_{39}](DMSO)$. *Cryst. Growth Des.* **2006**, *6*, 2266–2270.

41. Zhang, S.W.; Wang, Y.; Zhao, J.W.; Ma, P.T.; Wang, J.P.; Niu, J.Y. Two types of oxalate-bridging rare-earth-substituted Keggin-type phosphotungstates $\{[(\alpha-PW_{11}O_{39})RE(H_2O)]_2(C_2O_4)\}^{10-}$ and $\{(\alpha-x-PW_{10}O_{38})RE_2(C_2O_4)(H_2O)_2\}^{3-}$. *Dalton Trans.* **2012**, *41*, 3764–3772.

42. Wang, Y.; Sun, X.P.; Li, S.Z.; Ma, P.T.; Wang, J.P.; Niu, J.Y. Synthesis and magnetic properties of tartrate-bridging rare-earth-containing polytungstoarsenate aggregates from an adaptive precursor $[As_2W_{19}O_{67}(H_2O)]^{14-}$. *Dalton Trans.* **2015**, *44*, 733–738.

43. Barsukova, M.; Dickman, M.H.; Visser, E.; Mal, S.S.; Kortz, U. Synthesis and structural characterization of the yttrium containing isopolytungstate $[YW_{10}O_{36}]^{9-}$. *Z. Anorg. Allg. Chem.* **2008**, *634*, 2423–2427.

44. Ismail, A.H.; Dickman, M.H.; Kortz, U. 22-Isopolytungstate fragment $[H_2W_{22}O_{74}]^{14-}$ coordinated to lanthanide ions. *Inorg. Chem.* **2009**, *48*, 1559–1565.

45. Hussain, F.; Degonda, A.; Sandriesser, S.; Fox, T.; Mal, S.S.; Kortz, U.; Patzke, G.R. Yttrium containing head-on complexes of silico- and germanotungstate: Synthesis, structure and solution properties. *Inorg. Chim. Acta.* **2010**, *363*, 4324–4328.

46. Ibrahim, M.; Mal, S.S.; Bassil, B.S.; Banerjee, A.; Kortz, U. Yttrium(III)-containing tungstoantimonate(III) stabilized by capping, tetrahedral WO_4^{2-} unit, $[\{Y(\alpha-SbW_9O_{31}(OH)_2)(CH_3COO)(H_2O)\}_3(WO_4)]^{17-}$. *Inorg. Chem.* **2011**, *50*, 956–960.

47. Barsukova, M.; Izarova, N.V.; Ngo Biboum, R.; Keita, B.; Nadjo, L.; Ramachandran, V.; Dalal, N.S.; Antonova, N.S.; Carbó, J.J.; Poblet, J.M.; Kortz, U. Polyoxopalladates Encapsulating Yttrium and Lanthanide Ions, $[X^{III}Pd^{II}_{12}(AsPh)_8O_{32}]^{5-}$ (X = Y, Pr, Nd, Sm, Eu, Gd, Tb, Dy, Ho, Er, Tm, Yb, Lu). *Chem.-Eur. J.* **2010**, *16*, 9076–9085.

48. Kortz, U.; Savelieff, M.G.; Bassil, B.S.; and Dickman, M.H. A Large, Novel Polyoxotungstate $[As^{III}_6W_{65}O_{217}(H_2O)_7]^{26-}$. *Angew. Chem. Int. Ed. Engl.* **2001**, *40*, 3384–3386.

49. Brown, I.D.; Altermatt, D. Bond-valence parameters obtained from a systematic analysis of the Inorganic Crystal Structure Database. *Acta Crystallogr.* **1985**, *B41*, 244–247.

50. Thouvenot, R.; Fournier, M.; Franck, R.; Rocchiccioli-Deltcheff, C. Vibrational investigations of polyoxometalates. 3. Isomerism in molybdenum(VI) and tungsten(VI) compounds related to the Keggin structure. *Inorg. Chem.* **1984**, *23*, 598– 605.

51. Tourné, C.; Revel, A.; Tourné, G.; Vendrell, M. Heteropolytungstates containing elements of phosphorus family with degree of oxidation (iii) or (v)—identification of species having composition X_2W_{19} and XW_9 (X = P, As, Sb, Bi) and relation to those with composition XW_{11}. *C. R. Acad. Sci. Paris, Ser. C* **1973**, *277*, 643–645.

52. *SAINT*, Version 2.1-4; Bruker AXS Inc.: Madison, WI, USA, 2007.

53. Sheldrick, G.M. *SADABS*; Program for empirical absorption correction of area detector data; University of Göttingen: Göttingen, Germany, 1996

54. Sheldrick, G.M. *SHELX-97/2013*; Program for solution of crystal structures; University of Göttingen: Göttingen, Germany, 2013.